

The Effects of Austempering Heat Treatment Process Parameters on the Transformation Kinetics of Austenite to Bainite in AISI 52100 Steel

A Major Qualifying Project

Submitted to the Faculty of

Worcester Polytechnic Institute

In partial fulfillment of the requirements for the

Degrees of Bachelor of Science

By

Cory Houghton

John Hughes

Michael Nardo

Junaid Rathore

Matthew Robinson

Project Advisors:

Professor Richard D. Sisson, Jr

Professor Mei Yang

Table of Contents

Table of Contents	1
Table of Figures	3
Table of Tables	5
Abstract	6
Introduction	7
Literature Review	10
AISI 52100 Steel	10
Avrami Equation	12
Experimental Plan and Procedure	13
Sample Cutting	13
Heat Treatment	14
Sample Preparation	15
Polishing	16
Etching	16
Characterization	17
Optical Microscopy	17
Microhardness	17
Rockwell Hardness	17
Tint Etching	18
X-Ray Diffraction (XRD) Analysis	19
Experimental Results	20
240 °C Holding Temperature	20
Optical Microscopy	20
Microhardness	21
Rockwell Hardness	21
Tint Etching	22
XRD Analysis	23
230 °C Holding Temperature	25
Microhardness	25
Rockwell Hardness	25

Avrami Analysis (present the equation in lit review.	26
Discussion	27
Optical Microscopy	27
Tint Etching	27
Microhardness	28
Rockwell Hardness	29
Avrami Parameters	30
Conclusion	32
Appendix	34
References	42

Table of Figures

Figure 1: Graphical representation of the austempering process.	8
Figure 2: Time-Temperature-Transformation (TTT) diagram for 52100 steel.	9
Figure 3: Schematic of the cutting pattern used to obtain the samples for heat treatment.	12
Figure 4: Optical microscope images taken of austempered 52100 steel.	20
Figure 5: Optical microscope image showing a tint etched sample at 500x magnification.	21
Figure 6: Optical microscope image showing a tint etched sample at 500x magnification.	22
Figure 7: XRD analysis for samples austempered at 240 °C.	23
Figure 8: XRD analysis for samples austempered at 240 °C for various holding times.	23
Figure 9: Graph showing the microhardness for samples austempered at 230 °C.	24
Figure 10: Percent transformed for 240 °C and 230 °C based on TTT diagram/data	25
Figure 11: Microhardness table for 230 °C.	34
Figure 12: Optical micrographs of austempered samples at 1 minute holding time (240°C).	35
Figure 13: Optical micrographs of austempered samples at 2 minute holding time (240°C).	35
Figure 14: Optical micrographs of austempered samples at 5 minute holding time (240°C).	36
Figure 15: Optical micrographs of austempered samples at 10 minute holding time (240°C).	36
Figure 16: Optical micrographs of austempered samples at 20 minute holding time (240°C).	37
Figure 17: Optical micrographs of austempered samples at 30 minute holding time (240°C).	37
Figure 18: Optical micrographs of austempered samples at 40 minute holding time (240°C).	38
Figure 19: Optical micrographs of austempered samples at 50 minute holding time (240°C).	38
Figure 20: Optical micrographs of austempered samples at 70 minute holding time (240°C).	39

Figure 21: Optical micrographs of austempered samples at 80 minute holding time (240°C). 39

Figure 22: Optical micrographs of austempered samples at 90 minute holding time (240°C). 40

Figure 23: Optical micrographs of austempered samples at 120 minute holding time (240°C). 40

Figure 24: Optical micrographs of austempered samples at 160 minute holding time (240°C). 41

Table of Tables

Table 1: Chemical Composition of AISI 52100 Steel as Obtained from ASTM.	10
Table 2: Summary of Experimental Parameters.	14
Table 3: Summary of the Average Microhardness for 240 °C.	20
Table 4: Summary of the Rockwell Hardness for 240 °C.	20
Table 5: Summary of the Rockwell Hardness for 230 °C.	24
Table 6: Summary of the Calculated Avrami Parameters.	25
Table 7: Calculation of Percent Bainite from Rockwell Hardness Data.	30

Abstract

A series of experiments were conducted to determine the isothermal kinetics of the austenite to bainite transformation in 52100 steel at 230 and 240 °C. The steel was austenitized at 850 °C for 30 minutes and quenched in liquid salt. The percent Bainite was determined using a linearized relationship with HRC data, and qualitative data for the microstructure was determined using x-ray diffraction (XRD). It was found that the bainitic transformation started and finished earlier at 240 °C. The HRC data indicated a complete transformation at about 40 minutes for both 230 and 240 °C trials, but XRD for both showed retained austenite after these points. XRD data indicates no retained austenite after 80 minutes, implying a complete transformation at 80 minutes rather than at 40 minutes. The data was analyzed using the Avrami equation and was compared with TTT diagrams found in literature for 52100 steel. For 240 °C, N was determined to be 2 and K was determined to be $.011 \text{ min}^{-1}$. For 230 °C, N was determined to be 2.43 and K was determined to be $.0007 \text{ min}^{-1}$.

Introduction

A wide variety of steel alloys have been developed for use in specific applications. For each alloy, steel parts must be fabricated, and heat treated to meet the specifications. One heat treatment method for parts requiring both strength and toughness is austempering. Austempering is used in steels in order to produce bainite, a microstructure that has high yield and tensile strength, which proves useful in the industry today (Krishna et al. 2012)

A series of steel alloys have been developed for applications in bearings and the automotive industry (Kilicli & Kaplan, 2012, p.22). The austempering process requires process controls in both temperature and time. A typical austempering process is presented in Figure 1. During the first step of this process, the steel parts are heated into the austenite phase region and held until the austenite is uniform in temperature and chemical composition. The second step of the process requires the quenching of the part to an intermediate temperature which is above the martensite start (M_s) temperature. During the third step, the part is held constant at the temperature until a Bainitic microstructure is formed. Finally, the last step is cooling the part to room temperature.

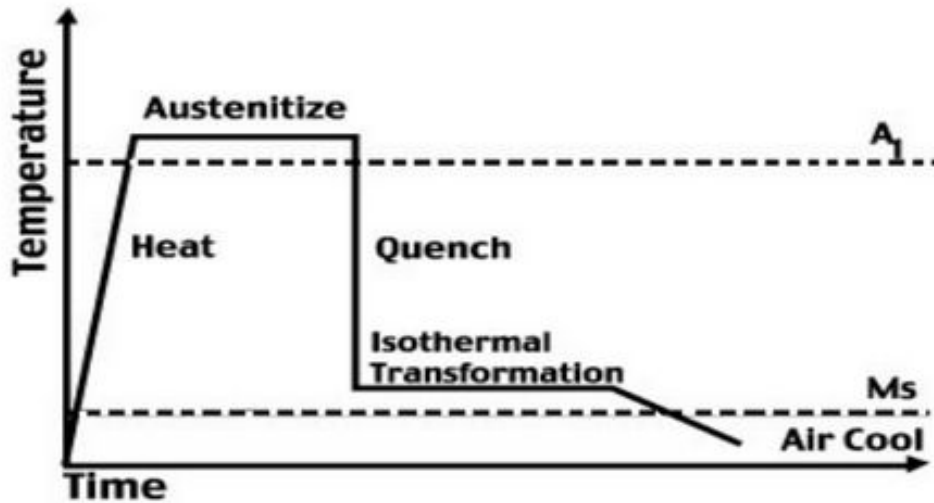


Figure 1: Graphical representation of the austempering process showing heating (Step 1), quenching to the intermediate temperature (Step 2), holding the temperature at the intermediate temperature (Step 3), and cooling to room temperature (Step 4) (Niazi, 2014).

In this process, the cooling rate in step 2 must be fast enough to avoid forming ferrite and/or pearlite. One of the key variables in this process is the media to quench into and hold the constant temperature. For this project molten salt was selected due to molten salt's unique characteristics such as its high boiling point and high thermal conductivity (Green et al.). During the austempering process the media must not evaporate. Molten salt is the most common choice of cooling media for austempering. Another important variable is the length of time of this isothermal heat treatment that will yield a 100% Bainitic microstructure. If the austempering holding time is not long enough, a mixed Bainitic and Martensitic with some retained austenite microstructure will result.

Type: 52100

Composition: Fe - 1.02% C - 0.36% Mn - 0.20% Ni - 1.41% Cr

Grain size: 9 Austenitized at 843°C (1550°F)

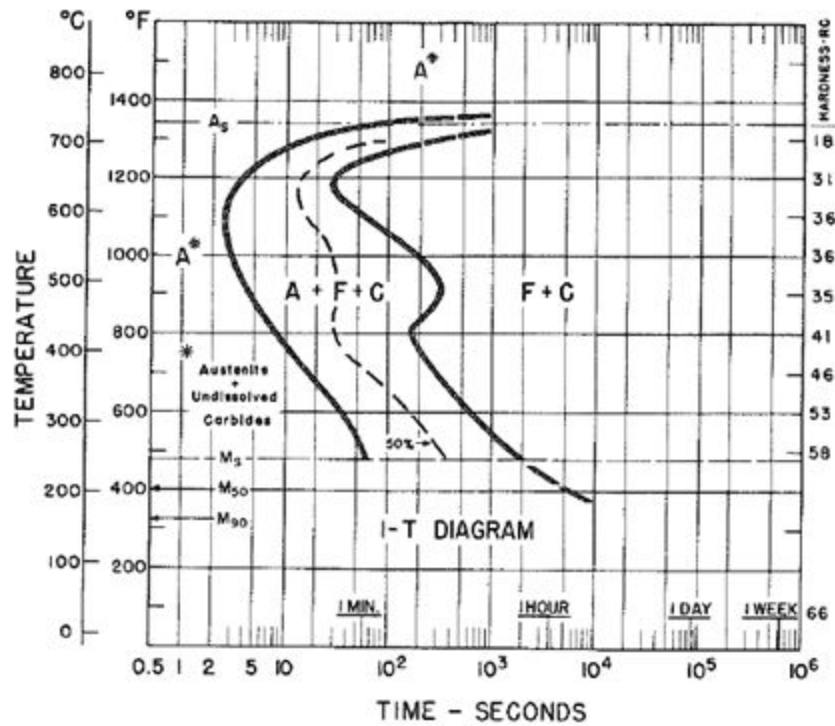


Figure 2: Time-Temperature-Transformation (TTT) diagram for 52100 steel (Vander Voort, 1991).

Therefore, a major goal of this project team is to determine the effects of isothermal hold times on the microstructure and mechanical properties of American Iron and Steel Institute (AISI) 52100 steel and to determine bainitic transformation kinetics in molten salt at selected austempering temperatures.

Literature Review

AISI 52100 Steel

AISI 52100 steel is a bearing steel with high carbon and chromium concentrations. The specific composition of AISI 52100 from the American Society for Testing and Materials (ASTM) is shown in the table below:

Table 1: Chemical composition of AISI 52100 steel as obtained from ASTM.

Element	C	Mn	P	S	Si	Cr	Mo	Ni	Cu	Al	Fe
wt. %	0.93- 1.05	0.25- 0.45	Max 0.025	Max 0.015	0.15- 0.35	1.35- 1.60	Max 0.10	Max 0.25	Max 0.30	Max 0.50	Bal.

The conventional heat treatment for 52100 is to quench and temper for a predominantly tempered-martensitic microstructure (Kilicli & Kaplan, 2012, p. 22). However, recent studies have shown that the mechanical properties of AISI 52100 can be improved using isothermal heat treatments such as austempering. The temperature and time of austempering have a great influence on the mechanical properties of AISI 52100, with studies showing that the austempering temperature has more of an impact than the austempering time. (Kilicli & Kaplan, 2012, p. 23).

The lower bainite microstructure formed by austempering AISI 52100 was found to be tougher with improved performance. (Hollox et al., 1981, p.889-893) Bainite has many advantages over tempered martensite, including higher yield strength with the same hardness as tempered steel, higher tensile stress, desirable compressive stresses at the surface, and improved notch impact strength. There is also less residual austenite than with martensitic hardening. (Kilicli & Kaplan, 2012, p.22). However, one disadvantage that bainitic formation has is the long dwell time which could make the process uneconomical.

Bainite hardening can be carried out using chamber furnaces or continuous lines. In the chamber furnace, an open or integrated salt bath is present acting as a sealed quench furnace. The austempering process begins with heating a sample to above the austenitizing temperature and rapidly cooling to just above the martensite start temperature, or M_s . Once the transformation is complete, the sample is cooled further to room temperature. The process design consists of determining the correct austenitizing and M_s temperature to austemper, as well as austempering holding times. Time-Temperature-Transformation (TTT) diagrams are conventionally used to design austempering process parameters since they show M_s temperatures and bainitic transformation start and finish times at specific austempering temperatures.

The M_s temperatures vary based on carbon concentration in the AISI 52100 after austenitizing. The carbon concentration in the austenite is correlated to the austenitization temperature and time. Since more carbides dissolve at higher austenitizing temperatures, the M_s temperature will decrease with the increase in carbon concentration. According to a previous

CHTE report on austempering bainite, the optimal austenitizing temperature to dissolve nearly all the carbon in AISI 52100 is above 900°C (Vander Voort, 1991).

Avrami Equation

The kinetics for the transformation were determined by the JMA equation, also known as the Avrami equation. This equation is based on two constants: K and n , and is written as $1 - \exp[-K \cdot t^n]$. The constant K is a temperature-dependent constant ($K(T) = K_0 \exp[-E/kt]$) and n is a constant typically varying between 1 and 4. Literature values from the TTT-diagram were taken at 1%, 50%, and 99% and plotted to get theoretical Avrami curves for the holding temperatures used. The data collected through experimental trials were also plotted and linearized to determine the experimental K and n (Ohring & Kasprzak, 2015).

Experimental Plan and Procedure

Table 2: Summary of Experimental Parameters.

Material	Austenitizing Temp (°C)	Austenitizing Time (min)	Austemperting Temp (°C)	Austemperting Time (min)
AISI 52100 (100Cr6)	850	30	240	10
				20
				40
				80
				160
			230	10
				20
				40
				80
				160

Sample Cutting

A 1.25 centimeter thick sample of AISI 52100 (spheroidized/carburized) steel was cut from a 5 centimeter diameter larger rolled steel rod parallel to its cross section using a power saw. This sample was then cut into quarters using a Mark V Series 600 Cutoff saw, and that

same saw was then used to cut each quarter into four pieces of similar size as described in Figure 3 below:

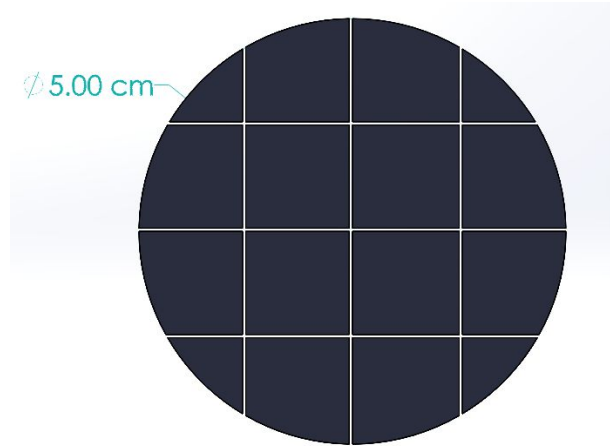


Figure 3: Schematic of the cutting pattern used to obtain the samples for heat treatment.

Heat Treatment

Two Thermolyne 30400 furnaces were used for the heat treatment of each 52100 steel sample. Both furnaces used thermocouples to ensure accurate temperature readings instead of relying on the temperature settings of the furnaces themselves. Thermocouples were calibrated using ice water and boiling water before being used in the furnaces to ensure proper temperature readings. The first furnace was set to 850 °C to austenize the sample, and the second furnace was set to an austempering temperature related to the experimental trial being conducted; either 240 °C, 230 °C or 220 °C.

Each sample was prepared for heat treatment by wrapping steel wire around the body of each sample, ensuring the sample was secure before being placed in the furnace. Each sample

was then lowered into the furnace via a small opening in the top of the furnace, and the samples were held there for 30 minutes to ensure complete austenitic transformation. A low temperature quenching salt was placed into a ceramic container and positioned inside the second furnace until the salt melted and came to the same temperature as the furnace.

The sample was placed in the 850 °C furnace for 30 minutes to ensure a uniform temperature and complete austenitic transformation. It was then quickly transferred from the first furnace into the molten salt bath within the 2nd furnace, once again through a small opening in the top of the furnace. The time each sample was held within the salt bath was varied, ranging from 1 minute to 160 minutes, with the full range of holding times available in Table 2. After being quenched in the molten salt bath for the specified amount of time, each sample was removed from the furnace and allowed to cool in air down to room temperature.

Sample Preparation

The samples were cut to expose the cross-section before mounting. Each sample, once cooled to room temperature, was placed individually in a plastic bag marked with the heat treating conditions of the sample. Each sample was then mounted using a Buehler Simplimet 4000 Mounting Press. Every sample was mounted using PhenoCure, and any sample planned for use with a Scanning Electron Microscope (SEM) also included a conductive phenolic compound at the surface of the mount in contact with the sample.

The mounting conditions for each sample were a 4 minute heating time at 4,400 psi and 450 °F, and each sample was cooled by the mounting press before being removed from the press.

Polishing

Each sample was polished using a Struers Tegramin-20 Polisher with polishing pads of 9, 3, and 1 μm grit, and polishing suspensions of Colloidal Silica. Once each sample was polished, it was placed sample-down into an orange plastic cover to prevent scratches, oxidation, and any other possible abrasions.

Etching

Chemical etching was performed on each sample using a 4 vol.% solution of nitric acid dissolved in denatured ethanol (nital). Etching was performed by adding a single drop of nital to the surface of the sample, which was then quickly hand manipulated to cover the entire surface of the sample. Water was rinsed over the top of the sample as soon as a change in color or clarity in the sample was noticed, and ethanol was then used to wash any remaining water off the sample to prevent corrosion and promote evaporation off the surface. The evaporation of the ethanol was accelerated by using a hair dryer to dry the sample, which was then either further etched if the color or clarity indicated an under-etch, or the sample was considered properly prepared for characterization and was placed back into the plastic orange cover.

Characterization

Optical Microscopy

After chemical etching, each sample was observed using an optical microscope at 500x and 1000x magnification. The microscope was connected to a camera, and 5 grayscale pictures were taken at each magnification for every sample. For each picture, a scale was added to assist in picture comparison between samples.

Microhardness

Samples were either characterized using microhardness before chemical etching, or after repolishing the etched surface as to avoid inconsistencies due to the etching. Microhardness relies upon accurate measurements of the diameter of indentation on a surface, and the lack of clarity on an etched surface makes the task of measuring that indentation more difficult and less accurate. Microhardness data was measured and recorded using a Wilson VH3300 Hardness Tester, which imprinted between 20-30 times in a straight line on the sample. Each indent was examined to ensure proper focus and then measured for the diameter of indentation to determine hardness, with every point then being averaged to determine overall microhardness of the sample.

Rockwell Hardness

All Rockwell Hardness characterizations were performed last on each sample due to the damage it causes to the metallic surfaces, and these tests were always performed on polished

surfaces rather than etched surfaces. Hardness testing was performed using a Wilson Rockwell Hardness Tester, which was calibrated using both a hard and soft metal of known hardness. 5 imprints were made on each sample, with care being taken to avoid any surface imperfections caused by the microhardness testing or other indents from Rockwell Hardness testing. Each imprint had its corresponding hardness recorded, and these values were then averaged and recorded as a singular value of hardness for each sample.

Tint Etching

Two chemical solutions were prepared for use in tint etching. The first was a 5% w/v solution of picric acid in ethanol, while the second was a 10% w/v solution of sodium metabisulfite in water. The picric acid solution was prepared using wetted picric acid for safety, which was then weighed out into a beaker to which an appropriate amount of distilled anhydrous ethanol was added. To this mixture, approximately 1 mL of concentrated lab grade hydrochloric acid was added per 100 mL of solution. The sodium metabisulfite solution was prepared by simply adding an appropriate amount of water to a measured amount of sodium metabisulfite.

Trials were conducted using 3 containers, one of which contained the picric acid solution, the other the sodium metabisulfite, and the third being a waste container due to the toxicity of picric acid not allowing for it to be put down the drain safely. Austempered samples were first held by tongs into the picric acid solution for approximately 40 seconds, after which it was transferred to the waste container to be rinsed by ethanol until none of the yellow color of the picric acid could be seen. Once the sample was fully rinsed, it was transferred to the sodium

metabisulfite solution via tongs and held for 7 seconds, after which it was rinsed with water, then ethanol, then dried. Due to the vibrant yellow color of the picric acid, any contamination into the sodium metabisulfite solution can easily be noted. The effects of this contamination are not known, but this contamination was avoided as much as possible via the rinsing step between solutions.

Viewing the etch under a microscope required a blue polarizing filter to be placed over the light source of the microscope before any color would be visible. A second colorless polarizing lens assembly was also used after the initial blue filter to control the amount of polarized light allowed to reach the sample. This second filter was able to be spun to either allow all light from the initial filter through or to block out nearly all of it, allowing for an adjustable clarity to the image and color.

X-Ray Diffraction (XRD) Analysis

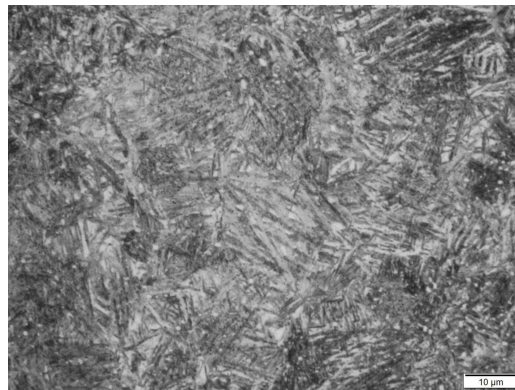
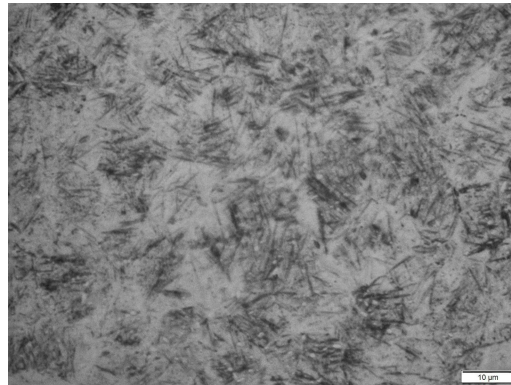
Each sample was tested using X-Ray Diffraction (XRD) in an attempt to identify the phases (martensite, retained austenite, bainite, etc.). Due to not being trained on the XRD, this portion of the characterization was performed by others. The results of the XRD characterization are presented later in this paper.

Experimental Results

240 °C Holding Temperature

Optical Microscopy

Optical comparisons of the different holding times indicated a maximum observable presence of bainite after approximately 40 minutes, after which each sampled holding time appeared nearly indistinguishable in terms of bainitic composition. In both the 40 and 80 minute optical micrographs, white cementite particles can also be seen in addition to the formed bainite.



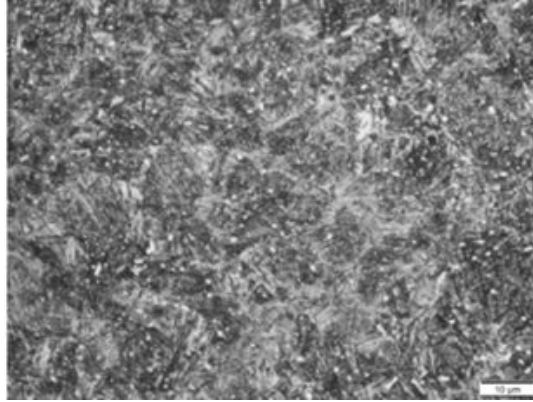


Figure 4: Optical microscope images taken of austempered 52100 steel. The first image is a sample that was austempered for 10 minutes, the second image is a sample that was austempered for 40 minutes and the third image is a sample that was austempered for 80 minutes. All three images were taken at 1000x magnification. The white particles are leftover cementite.

Microhardness

Table 3: Summary of the average microhardness for 10 minutes, 20 minutes, 40 minutes, 80 minutes and 160 minutes of austempering time at 240 °C.

Time	Microhardness
10	815.79
20	721.25
40	701.91
80	683.62
160	701.54

Rockwell Hardness

Table 4: Summary of the Rockwell hardness for 10 minutes, 20 minutes, 40 minutes, 80 minutes and 160 minutes of austempering time at 240 °C.

Time	Rockwell Hardness
10	59.76

20	56.38
40	53.44
80	53.44
160	52.78

Tint Etching

Tint etching was not able to be performed in a way which allowed for data to be gathered as to the generation of bainite at each holding time. Figure 5 and 6 below are two optical micrographs of a single 10 minute sample of 52100 after a holding temperature of 240 °C. Figure 5 and 6 are of the same image, but under different polarized lighting conditions, with the lighting on Figure 5 being considered more valuable for interpretation of bainitic transformation. Ultimately, no numerical data was able to be obtained from these initial stages of tint etching.

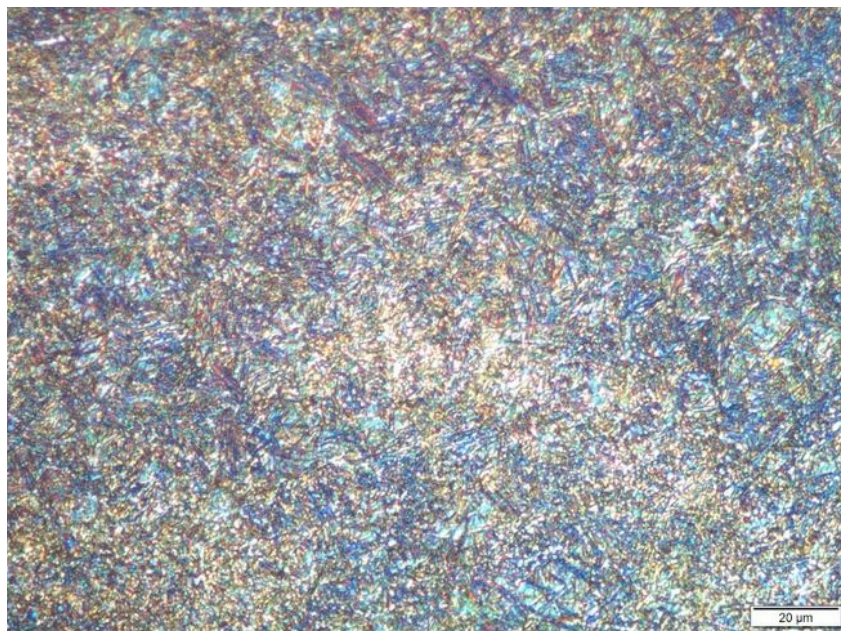


Figure 5: Optical microscope image showing a tint etched sample at 500x magnification. The sample was austempered at 240 °C for 10 minutes.



Figure 6: Optical microscope image showing a tint etched sample at 500x magnification. The sample was austempered at 240 °C for 10 minutes.

XRD Analysis

The results of the XRD analysis are presented in Figures 7 and 8 below. The main peak within each analysis corresponds to the combined peaks generated by martensite, bainitic ferrite, and 3 further peaks from cementite. A smaller peak can be observed far to the right of the main peak, corresponding to retained austenite (γ 220), which is seen to decrease in intensity as holding time increases, indicating a transformation from retained austenite to bainite.

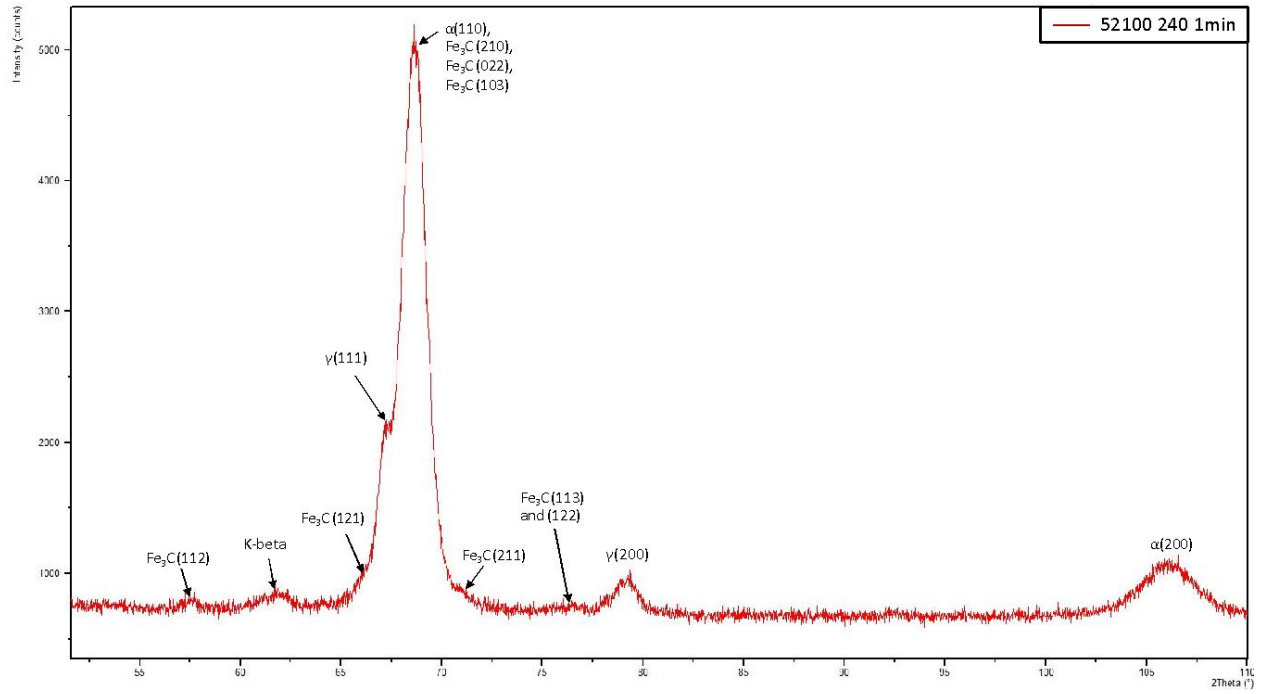


Figure 7: XRD analysis for samples austempered at 240 C.

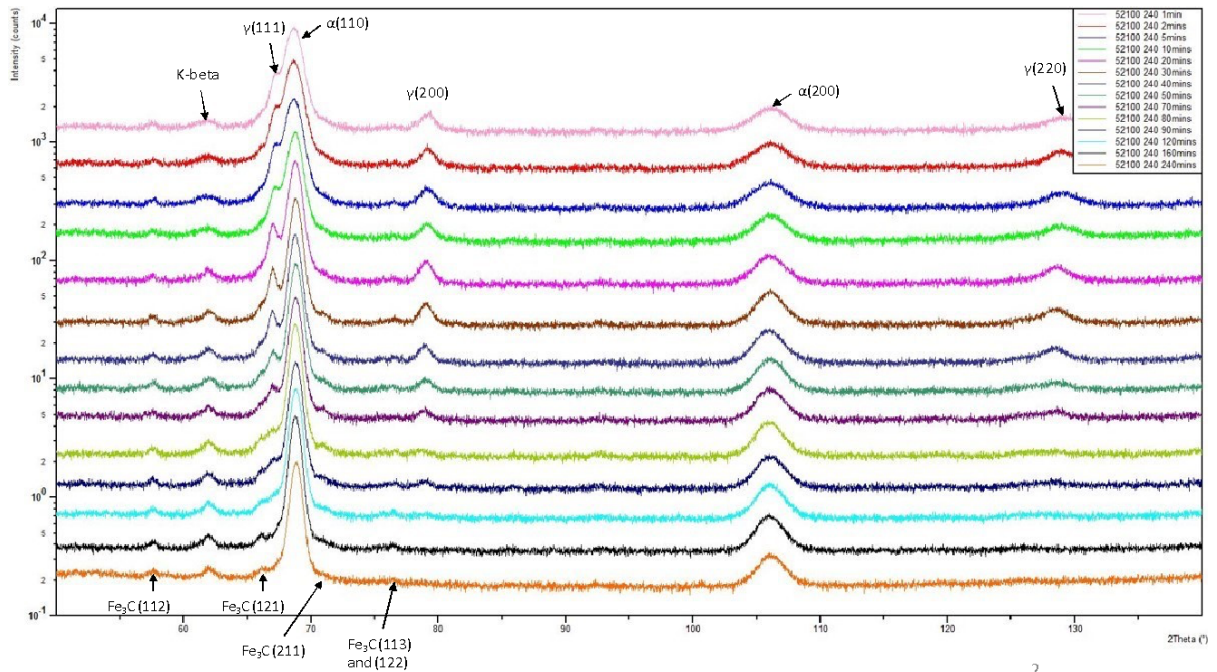


Figure 8: XRD analysis for samples austempered at 240 °C for various holding times.

230 °C Holding Temperature

Microhardness

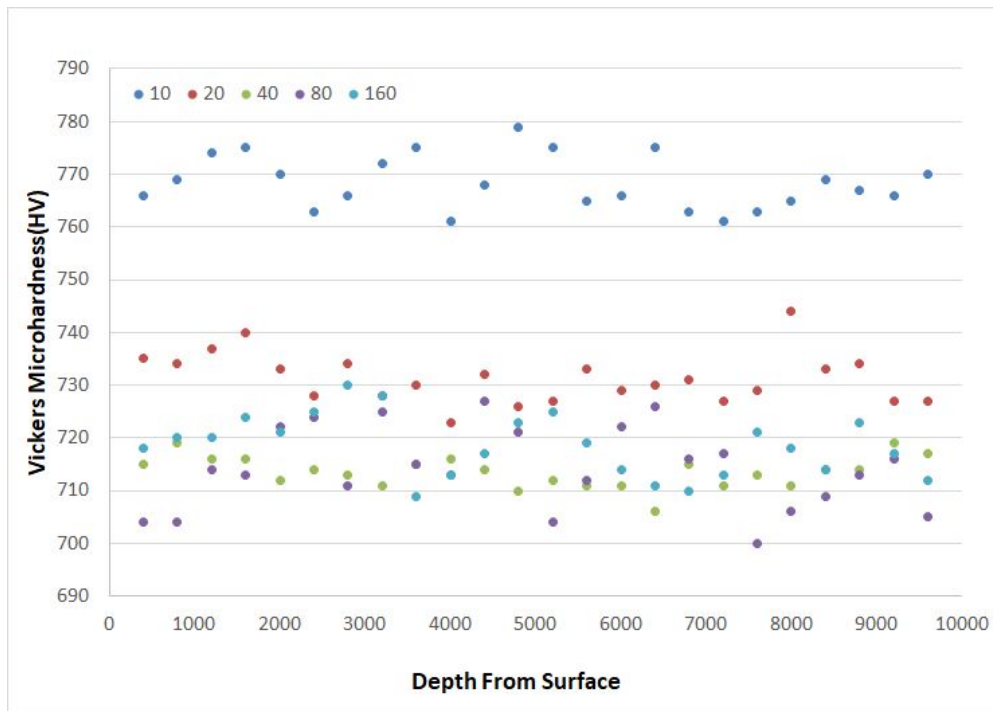


Figure 9: Graph showing the microhardness for samples austempered at 230 °C for various holding times.

Rockwell Hardness

Table 5: Summary of the Rockwell hardness for 10 minutes, 20 minutes, 40 minutes, 80 minutes and 160 minutes of austempering time at 230 °C.

Time	Rockwell Hardness
10	62.33
20	60.47
40	59.65
80	59.67

160	59.88
-----	-------

Avrami Analysis

Table 6: Summary of the calculated Avrami parameters based on theoretical and experimental results.

Trial Name	K (min ⁻¹)	N
240 °C TTT	.0133	1.76
230 °C TTT	.0106	1.64
240 °C Experimental	.011	2.00
230 °C Experimental	.0007	2.43

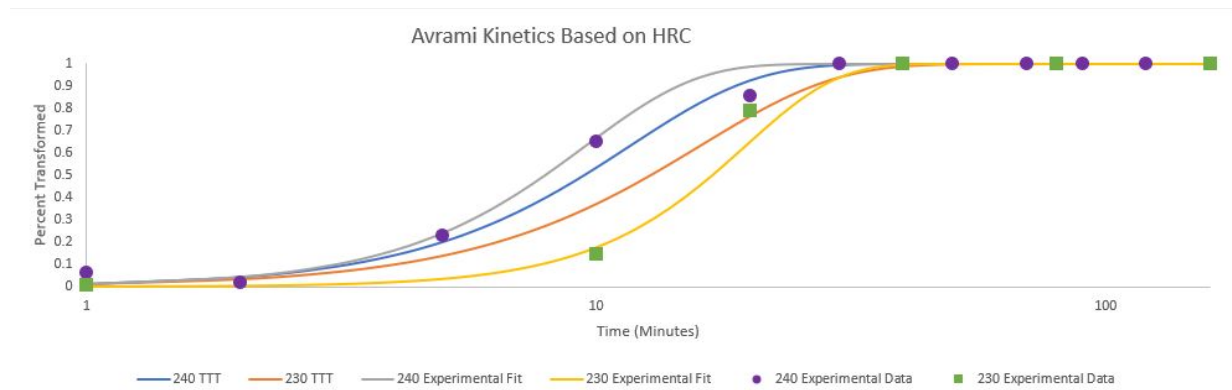


Figure 10: Graph showing the curves of percent transformed for 240 °C and 230 °C based on the TTT diagram and for 240 °C and 230 °C based on experimental results.

Discussion

Optical Microscopy

Optical microscopy was conducted on all 52100 samples austempered at 240 °C, and multiple images of each sample were captured at 500x and 1000x magnifications. A comparison of the images revealed that the amount of observable bainite increased drastically across the early holding times, then tapered off at approximately 30-40 minutes of holding time. Samples with a holding time greater than 40 minutes appeared virtually identical to each other, indicating that the bainitic transformation completes after 40 minutes austempering holding time.

Tint Etching

Data as to the composition of the 52100 steel samples at various holding times was not able to be determined from pictures taken after tint etching. This characterization step was still in its research and development step, and though it was planned to be used as another characterization method, the process was interrupted before this could occur. Instead, testing was done on samples in order to determine which method of tint etching revealed the clearest and most colorful image, as this would be vital for accurate analysis of any tint-etched samples. Several samples were etched according to the procedure documented in this report, but further testing was done on this procedure in some samples to determine if higher clarity could be achieved.

There were some unexpected complications which occurred while tint-etching on the first few samples. The main observed issue was that for some samples, the etch did not appear to be complete after a single etch, requiring two or even multiple etches for the proper appearance of an etch to take hold. An etch was considered to be adequate when it compared reasonably to that which was observed with the nital etching; a clouded surface with slight discoloration.

A second alteration which was used for one sample was to ignore the time a sample was in the picric acid solution and instead to hold the sample in solution until a surface change was observed. This test was performed on the 40 minute sample, and resulted from a total etch time of 60 seconds instead of 40. When the sodium metabisulfite solution was applied, the sample changed color far more than any other and looked much darker to the unaided eye. While other samples had a slight discoloration, this sample became much darker and light reflecting off of the surface was tinted blue and seemed slightly iridescent.

Microhardness

All available 52100 samples for the 240 and 230 °C holding temperatures were subject to microhardness characterization, though no samples for a 220 °C holding time were available or tested before the outbreak. The characterizations which were completed revealed a decreasing microhardness as holding time was increased, which can be attributed to the reduction of hard martensite in favor of softer bainite. This trend was expected to occur because the process of austempering is designed specifically to induce bainitic transformation, and the flattening of the curve between 20 and 40 minutes for both temperature samples indicates an approach to some upper limit of bainite concentration at those respective temperatures.

Rockwell Hardness

For both the 240 and 230 °C holding temperatures, hardness was observed to decrease as holding time increased. This was expected for the same reason that it was expected with microhardness, as the microhardness and hardness essentially measure the same phenomena, but with different methods. The Rockwell hardness tests showed diminishing results after approximately 40 minutes of holding time, indicating an approach to an upper limit of bainite after that time.

Rockwell hardness values were also used to determine the percent of bainite within each sample. A quenched sample was immediately placed into water after austenization in order to essentially generate 0% bainite and 100% martensite, though these values are idealized and in reality are likely not exact. This quenched sample was assumed to contain 0% bainite, while the 160 minute sample was assumed to be 100% bainite, allowing bainitic concentration to be derived as a linear function of time and hardness. The results for 240 and 230 °C experimental trials are outlined below in table 7. These percentages were further used for the determination of experimental Avrami parameters to describe the kinetics of bainite formation at these temperatures.

Table 7: Calculation of percent bainite from Rockwell hardness data for various times in the 240 and 230 °C austempering trials. Note, the bold values at 0 minutes and 160 minutes represent assumed values, while the bold values for 40 minutes and 80 minutes for the 230 °C trials represent theoretical values that exceed 100% bainite. The calculated composition values are given in parenthesis.

Time	Hardness (HRC) at 240 °C	Calculated Percent Bainite	Hardness (HRC) at 230 °C	Calculated Percent Bainite
0 Minutes (Quenched)	62.75	0.00%	62.75	0.00%
10 Minutes	59.76	29.99%	62.33	14.63%
20 Minutes	56.38	63.89%	60.47	79.44%
40 Minutes	53.44	93.38%	59.65	100.00% (108.01%)
80 Minutes	53.44	93.38%	59.67	100.00% (107.32%)
160 Minutes	52.78	100.00%	59.88	100.00%

Avrami Parameters

Graphing the Avrami equations under the parameters given by each trial revealed the relative speed of the kinetics at each temperature. Data obtained from time-temperature transformation curves obtained within the literature was also plotted on the diagram with the same temperatures as those tested.

For the 240 °C experimental data, parameters for the Avrami equation were first calculated as presented by the data, but the value for N was considered to be too low to be reasonable. Avrami curves are expected to be S shaped, necessitating the presence of an inflection point. The data gathered under the experimental trials for 240 °C did not reveal an

inflection point because this point only occurs at values of $N \geq 1$, while the calculation for N was found to be .5 and the calculation of K was .064. This low value of N , instead of creating an S curve, instead created a curve which was concave down at every point and showed no inflection, resulting in a curve that did not compare well to the experimental data. Due to the low value of N , an N parameter was instead assumed to be 2, due to this being a common value for several different transformations, and a K value was calculated to best fit the data. The assumption for $N = 2$ is also supported by the other data obtained during this experiment, as the other curves which were fit all had N values close to this number. The newly fitted plot gave a new value of 2 for N and $.011 \text{ min}^{-1}$ for K , and also resulted in a curve with a characteristic S shape. The 240°C experimental curve appeared sooner than any other curve, indicating faster kinetics at this temperature. When compared to the TTT diagram curve for 240°C , the experimental results were slightly faster than expected from the literature.

For the 230°C experimental data, the curve fitting did not run into the same difficulties presented by the 240°C data. The 230°C data was fit with a K value of $.0007 \text{ min}^{-1}$ and an N value of 2.43. This curve appeared after both the TTT and experimental 240°C curves, and also appeared after the 230°C TTT curve, indicating slower kinetics than would have been expected in the literature. While the experimentally determined kinetics were slower than expected based on literature values, the expectation that 240°C transformation would occur faster than 230°C transformations based on the TTT diagram appeared consistent with experimental results.

Conclusion

Avrami analysis performed over the course of this experiment showed that bainitic transformation began sooner for 240 °C than expected with respect to literature values obtained from TTT diagrams for 52100 steel, while 230 °C appeared to initiate slightly slower than literature values would indicate. Essentially, the experimentally measured transformations start sooner than the data from the TTT diagram (Vander Voort, 1991) at 240 °C while later at 230 °C.

The Avrami kinetics, which were able to be gathered over the course of this experiment, were measured under the assumption that the upper and lower limits of HRC measurements on each sample corresponded to a 0 and 100% transformation into bainite. This assumption was necessary in order to calculate a percent transformation from austenite into bainite, but does not necessarily represent the whole of the reality in respect to this type of transformation. If the transformation of bainite is incomplete, martensite will form from the retained austenite on cooling to room temperature. Specifically, the XRD analysis performed over each holding time details some fraction of retained austenite as being present far after hardness testing would indicate a 100% transformation into bainite, implying that hardness data alone is not sufficient to determine bainitic concentration.

Unfortunately, XRD analysis was also unable to determine bainitic transformation at these holding temperatures due to the presence of cementite in the microstructure and overlapping peaks of cementite and ferrite. In order to measure the fractions of bainite, the peaks must be deconvoluted to determine each phase's contribution to the overall peak. With the additional 3 cementite peaks contributing to the singular main peak, this data becomes nearly

impossible to decipher, but the data is still able to clearly show that the sample is not uniformly bainite at the holding times which HRC and optical microscopy indicated it would be.

XRD may become more useful for determining bainitic concentration in future experiments run at higher holding temperatures, as these temperatures might result in the dissolution of carbides and thereby the removal of cementite from the main peak, allowing for deconvolution of the data. Unfortunately, holding times at these higher temperatures would likely be longer than the times used over the course of this experiment due to the nature of bainitic transformation outlined by the TTT diagrams in the literature, as kinetics are not expected to increase in rate uniformly as temperature increases due to the reduction in driving force at higher temperatures.

Appendix

	10	20	40	80	160
400	766	735	715	704	718
800	769	734	719	704	720
1200	774	737	716	714	720
1600	775	740	716	713	724
2000	770	733	712	722	721
2400	763	728	714	724	725
2800	766	734	713	711	730
3200	772	728	711	725	728
3600	775	730	715	715	709
4000	761	723	716	713	713
4400	768	732	714	727	717
4800	779	726	710	721	723
5200	775	727	712	704	725
5600	765	733	711	712	719
6000	766	729	711	722	714
6400	775	730	706	726	711
6800	763	731	715	716	710
7200	761	727	711	717	713
7600	763	729	713	700	721
8000	765	744	711	706	718
8400	769	733	714	709	714
8800	767	734	714	713	723
9200	766	727	719	716	717
9600	770	727	717	705	712
mean	768.458	731.292	713.542	714.125	718.542

Figure 11: Microhardness table for 230 °C samples.

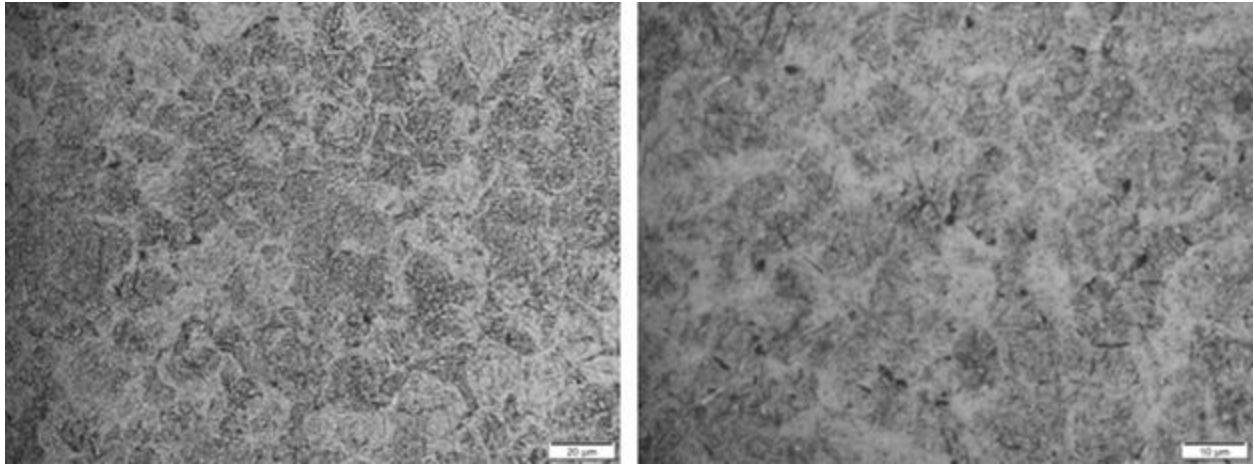


Figure 12: Optical micrographs of austempered samples of 52100 steel at 1 minute holding time (240 C).

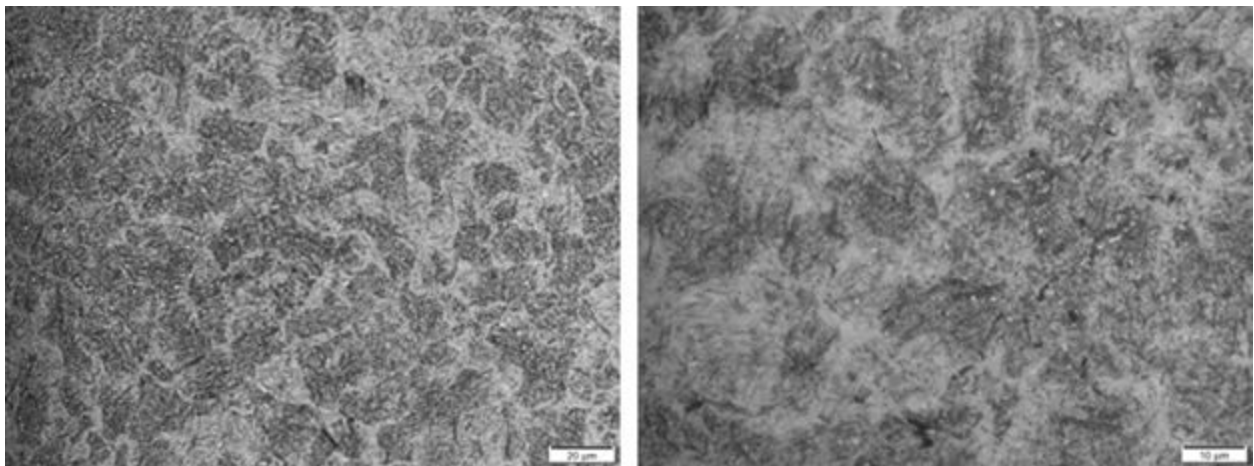


Figure 13: Optical micrographs of austempered samples of 52100 steel at 2 minute holding time (240 C).

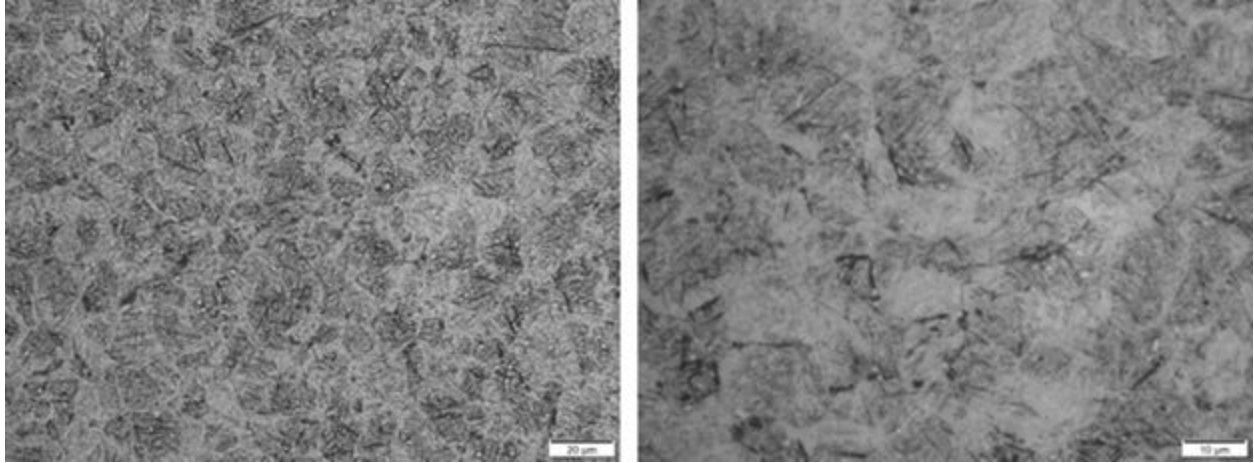


Figure 14: Optical micrographs of austempered samples of 52100 steel at 5 minute holding time (240 C).

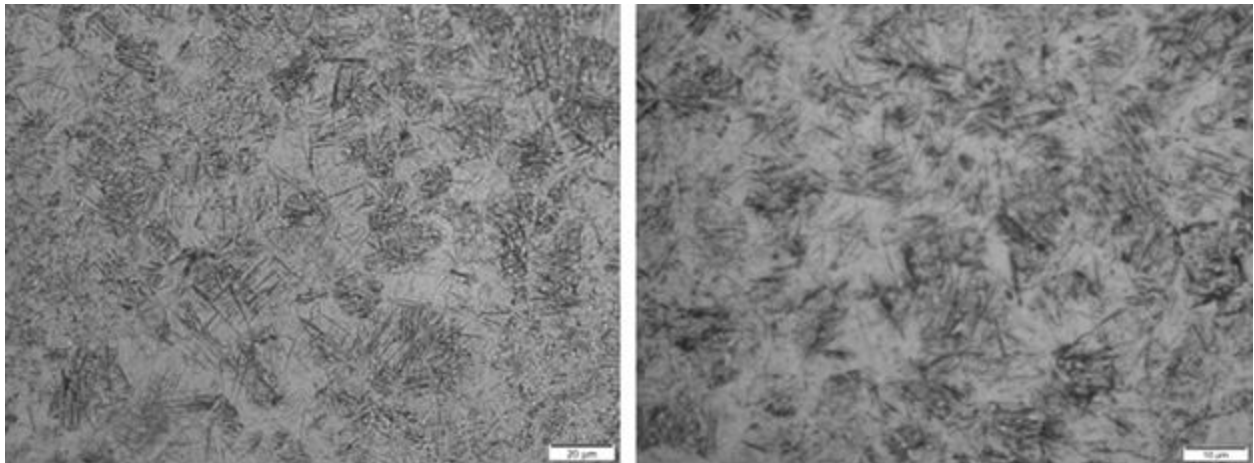


Figure 15: Optical micrographs of austempered samples of 52100 steel at 10 minute holding time (240 C).

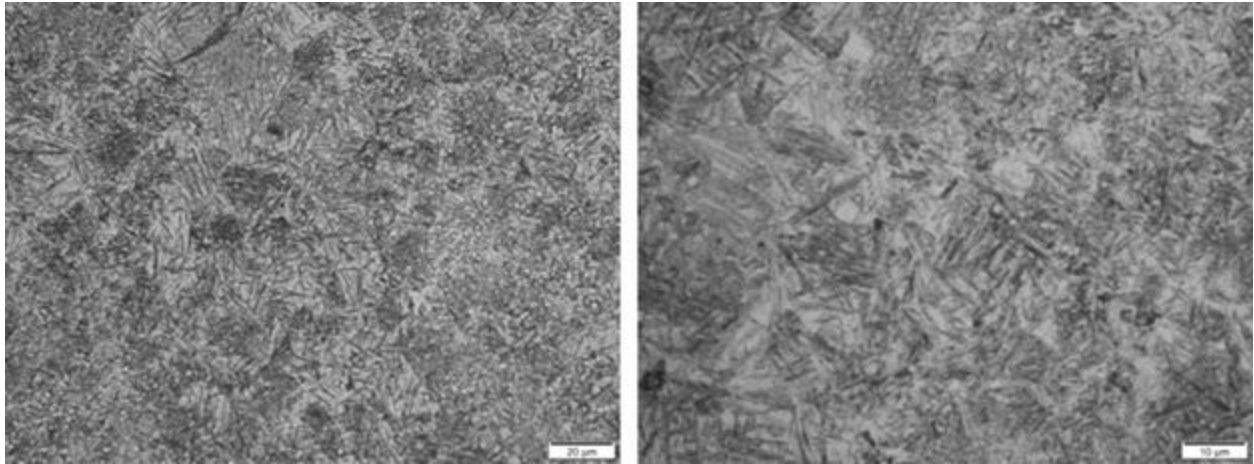


Figure 16: Optical micrographs of austempered samples of 52100 steel at 20 minute holding time (240 C).

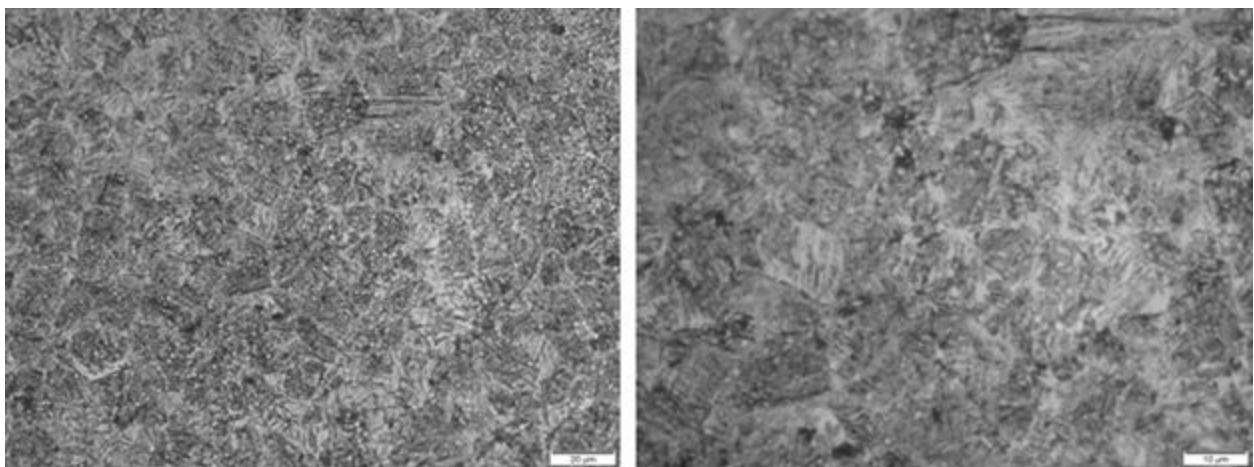


Figure 17: Optical micrographs of austempered samples of 52100 steel at 30 minute holding time (240 C).

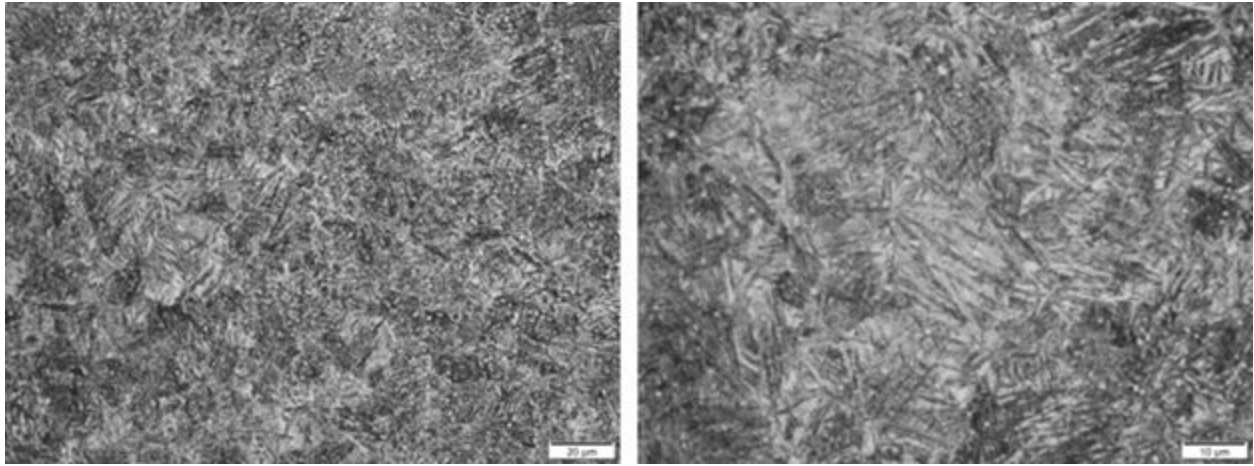


Figure 18: Optical micrographs of austempered samples of 52100 steel at 40 minute holding time (240 C).

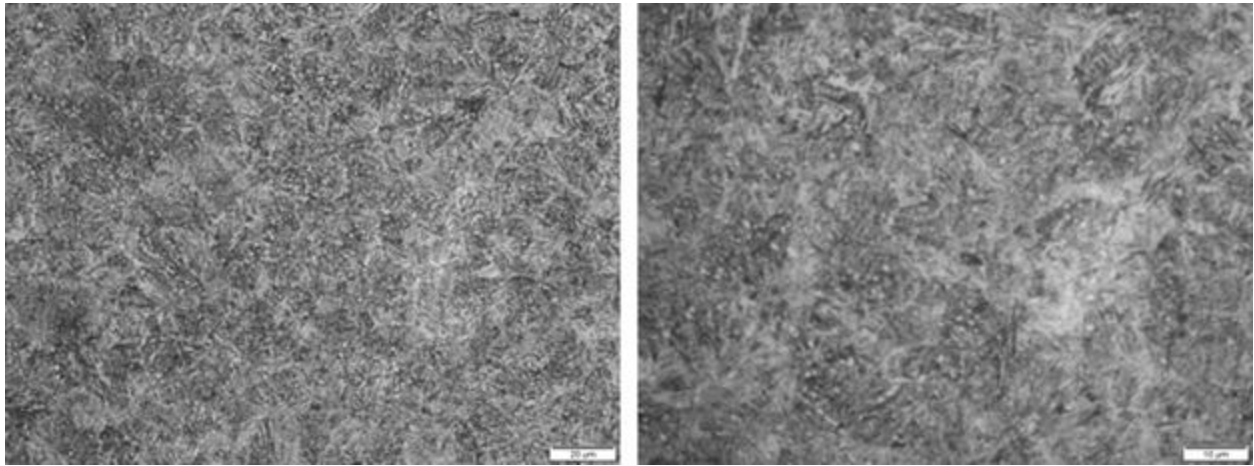


Figure 19: Optical micrographs of austempered samples of 52100 steel at 50 minute holding time (240 C).

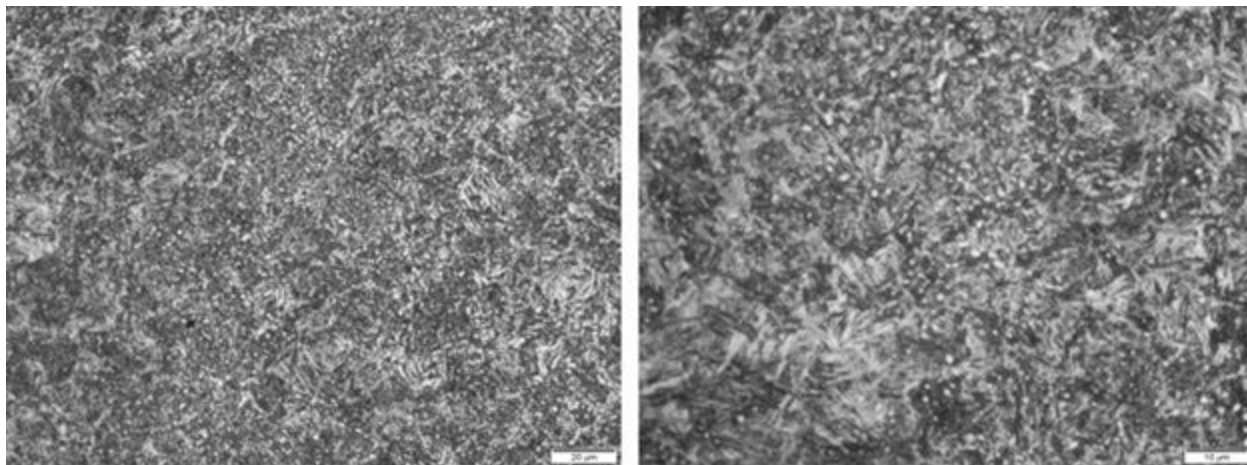


Figure 20: Optical micrographs of austempered samples of 52100 steel at 70 minute holding time (240 C).

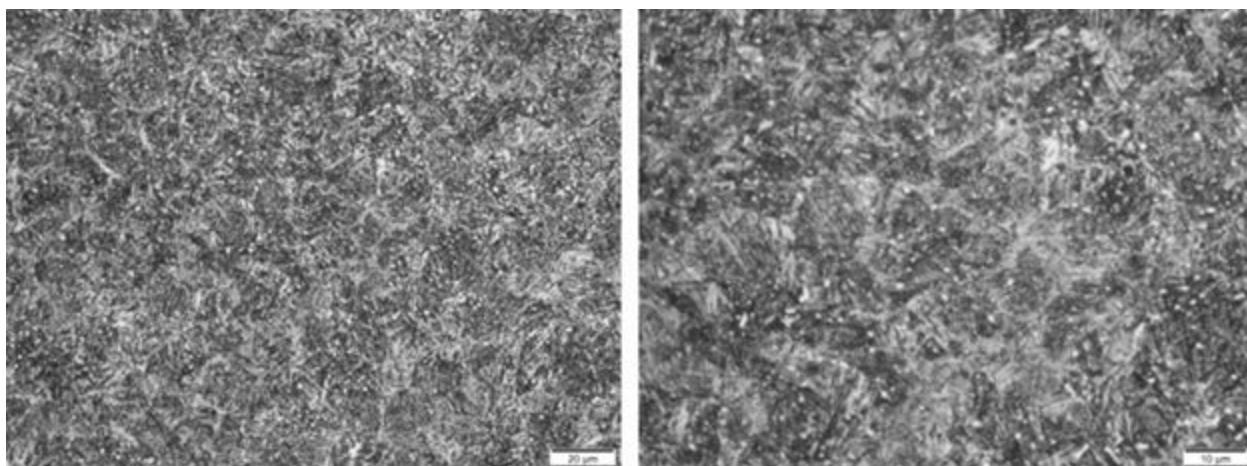


Figure 21: Optical micrographs of austempered samples of 52100 steel at 80 minute holding time (240 C).

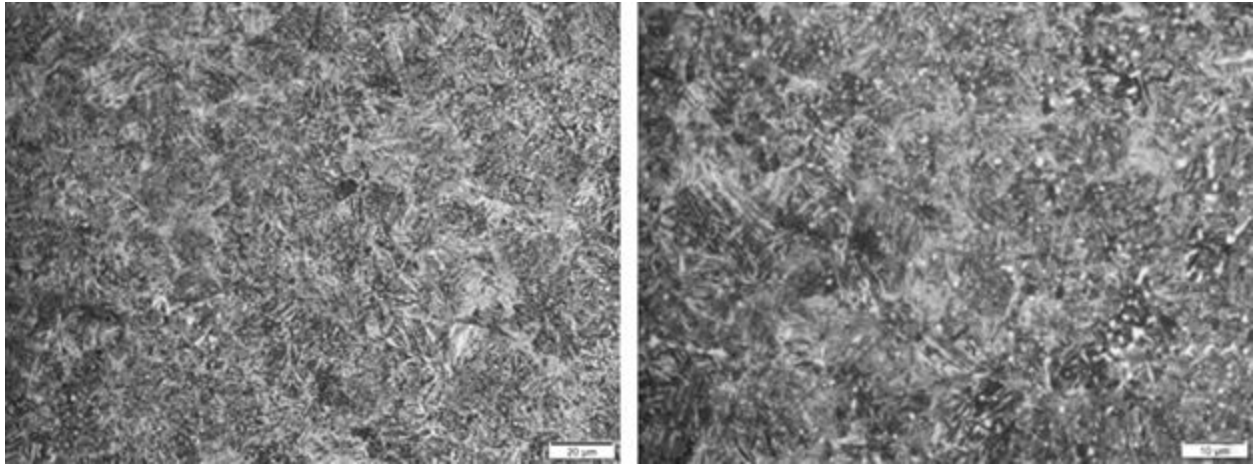


Figure 22: Optical micrographs of austempered samples of 52100 steel at 90 minute holding time (240 C).

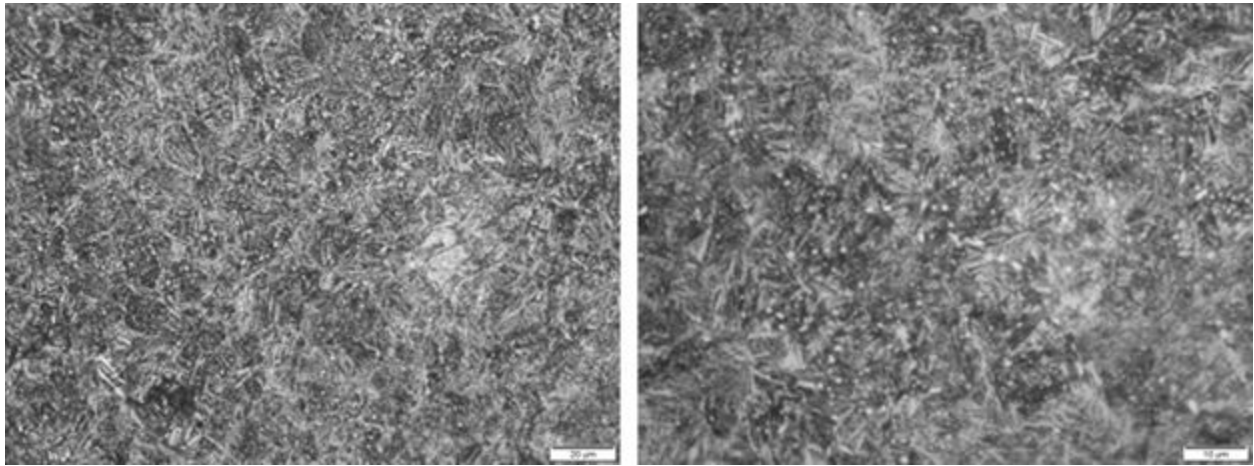


Figure 23: Optical micrographs of austempered samples of 52100 steel at 120 minute holding time (240 C).

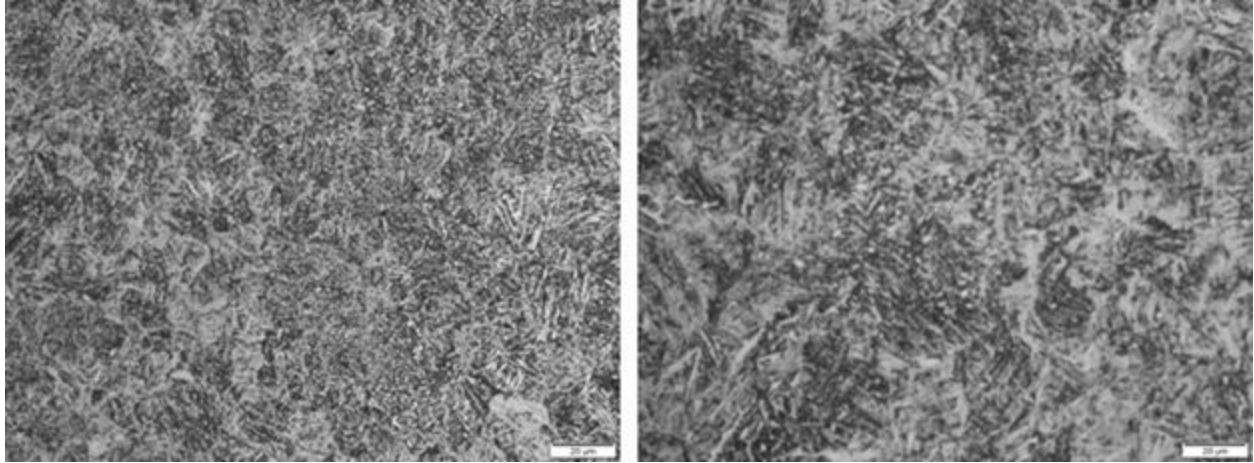


Figure 24: Optical micrographs of austempered samples of 52100 steel at 160 minute holding time (240 C).

References

- Akbasoglu, F. C., & Edmonds, D. V. (1990). Rolling contact fatigue and fatigue crack propagation in 1C-1.5Cr bearing steel in the bainitic condition. *Metallurgical Transactions A*, 21(3), 889–893. doi: 10.1007/bf02656572
- Hollox, G., Hobbs, R., & Hampshire, J. (1981). Lower bainite bearings for adverse environments. *Wear*, 68(2), 229–240. doi: 10.1016/0043-1648(81)90091-0.
- Kilicli, V., & Kaplan, M. (2012, September). EFFECT OF AUSTEMPERING TEMPERATURES ON MICROSTRUCTURE AND MECHANICAL PROPERTIES OF A BEARING STEEL.
- Krishna, Vamsi, P., Srikant, Iqbal, Mustafa, & Sriram. (2012, August 15). Effect of Austempering and Martempering on the Properties of AISI 52100 Steel.
- Niazi, N., & Shah, A. (2014, October). Austempering Heat Treatment of AISI 4340 Steel and Comparative Analysis of Various Physical Properties at Different Parameters.
- Nuclear Hybrid Energy System- Molten Salt Energy Storage by Michael Green, Piyush Sabharwall, Michael George Mckellar, Su-Jong Yoon, Cal Abel, Bojan Petrovic and Daniel Curtis
- Ohring, M., & Kasprzak, L. (2015). Avrami Equation. Retrieved May 06, 2020, from <https://www.sciencedirect.com/topics/engineering/avrami-equation>
- Sisson, R. D., Smith, R. C., Wang, Y., Yang, M., You, H., Yu, H., & Zhang, Y. (2019). Austempering to Form Bainite. *Austempering to Form Bainite*.
- Vander Voort, G. F. (1991). *Atlas of time-temperature diagrams for irons and steels*. S.L.: ASM International.